

Demonstration of Probabilistic-Based Durability Analysis Method for Metallic Airframes

J. N. Yang*

George Washington University, Washington, DC
and

S. D. Manning†

General Dynamics, Fort Worth Division, Fort Worth, Texas

Two different variations of a probabilistic-based durability analysis method are demonstrated and evaluated for countersunk fastener holes in the lower wing skin (7475-T7351 aluminum) of a fighter aircraft. The initial fatigue quality of the fastener holes is represented by an equivalent initial flaw size (EIFS) distribution. Probability of crack exceedance predictions at any service time are based on an EIFS distribution and two different service crack growth approaches. The service crack growth is divided into two segments. Segment 1 covers the small crack size region (e.g., <1.27 mm) and segment 2 the large crack size region (e.g., >1.27 mm). Approach I treats the service crack growth as deterministic for both segments. In approach II, the service crack growth is treated as deterministic in segment 1 and stochastic in segment 2. Analytical predictions for the extent of damage (i.e., number of fastener holes exceeding specified sizes), based on approaches I and II, are compared and correlated with experimental results. Good correlations are obtained for both approaches. Approach II was found to be more conservative than approach I.

Nomenclature

a_0	= reference crack size
$a(0)$	= EIFS at time $t = 0$
$a(t)$	= crack size at time t
AL, AU	= lower and upper bound crack sizes, respectively, defining the range of fractographic data used for determining EIFS
b_1, b_2	= crack-growth-rate exponents for crack growth segments 1 and 2, respectively ($b_1 = b_2 = 1$; used herein)
$f_X(u)$	= probability density function of the lognormal random variable X
$F_{a(0)}(x)$	= cumulative distribution function for EIFS
$F_{a(\tau)}(x_1)$	= cumulative distribution of crack size at any service time τ
$F_{T(x_1)}(\tau)$	= cumulative distribution of service time to reach any crack size x_1
$\bar{L}(\tau)$	= average number of details in the entire component having a crack size exceeding x_1 at any service time τ
N_i	= number of details in the i th stress region
$\bar{N}(i, \tau)$	= average number of details in the i th stress region having a crack size exceeding x_1 at any service time τ
$p(i, \tau)$	= probability that a detail in the i th stress region will have a crack size $> x_1$ at the service time τ
P	= probability
Q	= crack-growth parameter

Q_i	= service crack-growth parameter for the i th stress region
Q_1, Q_2	= crack-growth-rate parameters for service crack growth segments 1 and 2, respectively
$T(x_1)$	= service time to reach any crack size x_1
X	= lognormal random variable with a median value 1
x_u	= upper bound limit for EIFS
Z	= $\ln X$ (normal random variable)
σ	= gross section stress
σ_i	= maximum stress level in the i th stress region
$\sigma_L(\tau)$	= standard deviation of $L(\tau)$
σ_z	= standard deviation of $Z = \ln X$; a measure of the crack growth life dispersion
ξ, ψ	= empirical constants in equation: $Q_i = \xi \sigma_i^\psi$

Introduction

THE U.S. Air Force has damage tolerance¹⁻⁴ and durability^{1,2,4} design requirements for metallic airframes. Damage tolerance requirements are concerned with structural safety, which is usually governed by selected structural details (e.g., fastener holes, lugs, fillets, cutouts, etc.) in a part of a component. Durability requirements are concerned with minimizing functional impairment, such as excessive cracking (e.g., cracks < 2.54 mm), fuel leaks, and ligament breakage. Airframe durability affects structural maintenance requirements, economic life, and operational readiness. A metallic airframe contains thousands of structural details, and all such details are susceptible to fatigue cracking in service. Therefore, a statistical approach is essential for durability analysis to quantitatively estimate the extent of damage (i.e., number of details expected to exceed specified crack size limits) at any service time.

A damage tolerance design handbook⁵ is available for ensuring damage tolerance requirements. Probabilistic-based durability analysis "design tools" have been developed recently for ensuring the Air Force's durability design requirements for metallic airframes. These methodologies are documented in the Air Force's durability design handbook⁶ and elsewhere.⁷⁻¹⁹ The methodologies have been demonstrated and verified for fastener holes in coupon specimens and full-scale

Presented as Paper 88-2421 at the AIAA/ASME/ASCE/AHS 29th Structures, Structural Dynamics and Materials Conference, Williamsburg, VA, April 18-20, 1988; received May 23, 1988; revision received Aug. 28, 1989. Copyright © 1988 American Institute of Aeronautics and Astronautics, Inc. All rights reserved.

*Professor; currently on sabbatical leave at Institute of Aeronautics and Astronautics, National Chen Kung University, Tainan, Taiwan, ROC.

†Engineering Specialist Senior.

aircraft structure for a wide range of crack sizes covering functional impairment concerns.

Two different two-segment, crack-growth approaches have been recommended for performing durability analysis in both the small and large crack size regions.^{12,13} These two crack-growth approaches are referred to as 1) the "two-segment deterministic crack growth approach," or approach I; and 2) the "two-segment deterministic-stochastic crack growth approach," or approach II. Both approaches have been evaluated for both small and large fatigue cracks in clearance-fit, straight-bore, and countersunk fastener holes in 7475-T7351 aluminum.¹⁴

The purpose of this paper is to compare, evaluate, and demonstrate two different two-segment crack growth approaches (i.e., approach I and II) for predicting statistically the extent of cracking in a durability-critical component associated with fuel leaks and ligament breakage (e.g., crack size 12.7 mm to 19.0 mm). Both approaches are demonstrated using fractographic results from dog-bone specimens to predict the extent of damage in full-scale lower wing skins of a fighter aircraft. Analysis procedures and essential details are presented. Further details and equation derivations are given elsewhere.^{6,13,14}

Technical Approach

Two different approaches are conceptually described in Fig. 1. For both approaches, the initial fatigue quality of structural details is represented by an equivalent initial flaw size (EIFS) distribution. Once the EIFS distribution has been defined, a service crack-growth curve is used to grow the EIFS distribution from service time $t = 0$ to any service time. The service crack growth curve is divided into two different crack-growth segments to permit an accurate representation of the

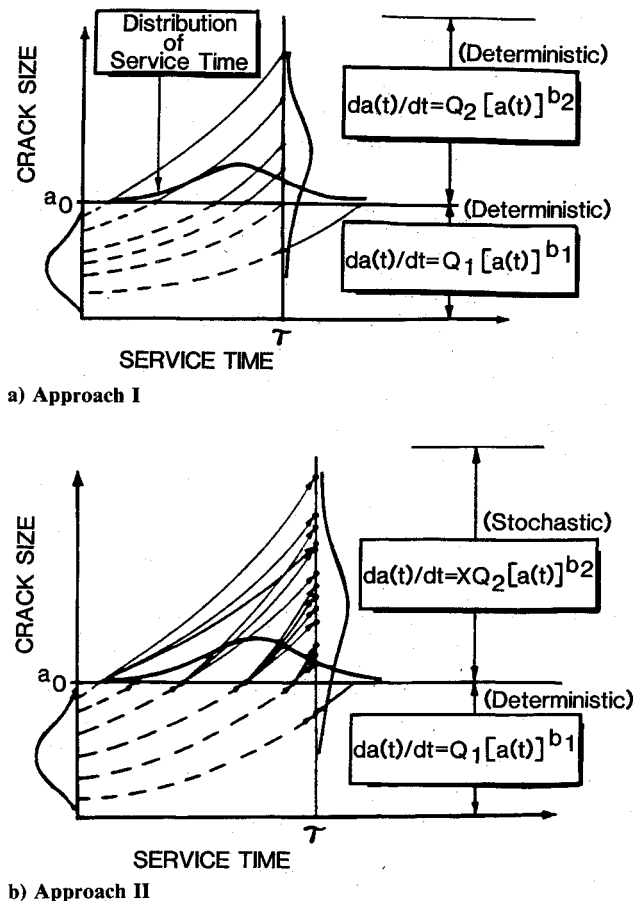


Fig. 1 Two-segment crack-growth approaches for durability analysis.

service crack growth curve for a wide range of crack sizes. For crack sizes $\leq a_0$, the service crack growth is treated as deterministic. For larger crack sizes, the service crack growth is treated as deterministic or stochastic. Service crack-growth trajectories are depicted in Figs. 1a and 1b for approaches I and II, respectively.

Initial Fatigue Quality

The initial fatigue quality defines the initially manufactured state of a structural detail or details with respect to initial flaws in a part, component, or airframe prior to service. For a group of replicate details (e.g., fastener holes), it is represented by an EIFS distribution. An equivalent initial flaw is an artificial initial crack size, which results in an actual crack size at an actual point in time when the initial flaw is grown under service crack growth conditions.

The Weibull compatible distribution function proposed by Yang and Manning^{15,16} has been found to be reasonable for representing the EIFS cumulative distribution⁶⁻¹⁶

$$F_{a(0)}(x) = \exp \left\{ - \left[\frac{\ln(x_u/x)}{\phi} \right]^\alpha \right\}; \quad 0 \leq x \leq x_u$$

$$= 1.0; \quad x > x_u \quad (1)$$

in which x_u = EIFS upper bound limit; α and ϕ are distribution parameters.

An EIFS value for a fastener hole is determined by back-extrapolating fractographic data in a selected crack size range ($AL - AU$) using a simple but versatile deterministic crack-growth rate model recommended by Yang and Manning^{15,16}

$$da(t)/dt = Qa(t) \quad (2)$$

where $da(t)/dt$ = crack-growth rate, $a(t)$ = crack size at any time t in flight hours, and Q is a crack-growth-rate parameter. Equation (2) ensures that all EIFS values are positive.¹³ It has been shown that EIFS values can be defined by back-extrapolation of fractographic data using either a deterministic^{6-9,12-16} or a stochastic^{10,14} crack growth law. However, the deterministic crack-growth law given by Eq. (2) was recommended for simplicity as well as some other reasons (see Refs. 6, 13, and 14).

After EIFS values $a(0)$ are obtained from all available fractographic data in the crack-size range $AL-AU$, they are fitted by Eq. (1) to determine the EIFS distribution parameters x_u , α , and ϕ . To predict the extent of cracking in service, the initial flaw size distribution Eq. (1) is grown forward to derive the statistical distribution of the crack size $a(t)$ at any service time t . Then, the following quantities can be predicted: 1) the probability that a crack in the i th stress region at any service time τ will exceed any given crack size x_i denoted by $p(i, \tau)$ and 2) the cumulative distribution of service time, $F_{T(x_i)}(\tau)$ for a crack in the i th stress region to reach any given crack size x_i . The $p(i, \tau)$ is referred to as the crack exceedance probability.

Two-Segment Crack Growth Damage Accumulation in Service

After the EIFS distribution given by Eq. (1) is determined, it is grown forward using a service crack-growth curve (SCGC) for a given stress region. The SCGC in each stress region is determined by either available fractographic results or a linear, elastic, fracture-mechanics, crack-growth-analysis computer program.^{13,14} To simplify the durability analysis procedures, the SCGC is fitted by analytical crack-growth equations. To obtain a reasonable fit, the SCGC is divided into two segments: one with the crack size smaller than the reference crack size a_0 (where $AL < a_0 \leq AU$) at crack initiation and the other with the crack size larger than a_0 .

A deterministic analytical crack-growth-rate equation is used to fit the first segment of the SCGC where the crack size is smaller than a_0 ,

$$da(t)/dt = Q_1[a(t)]^{b_1}; \quad a(t) \leq a_0 \quad (3)$$

The reason for using a deterministic rather than a stochastic crack growth equation [Eq. (3)] for the first segment is that the EIFS values were obtained by back extrapolation of fractographic data in the small crack size region using a deterministic, crack-growth equation [Eq. (1)]. Hence, any service, crack-growth curve in the small crack-size region should be compatible with the EIFS values, i.e., deterministic back extrapolation and deterministic crack growth in the small crack-size region (for detailed discussions, see Refs. 6, 13, and 14).

For the second segment of the SCGC, where the crack size is larger than a_0 , either a deterministic or a stochastic, crack-growth equation can be used. When a deterministic, crack-growth equation is used for the second segment of the SCGC, it is referred to as the two-segment deterministic, crack-growth approach (approach I). On the other hand, when a stochastic, crack-growth equation is used, it is referred to as the two-segment deterministic-stochastic, crack-growth approach (approach II). Approach I and approach II are schematically shown in Figs. 1a and 1b, respectively.

Two-Segment Deterministic Crack-Growth Approach (Approach I)

In this approach, a deterministic crack-growth equation is fitted to the second segment of the SCGC, where the crack size is larger than a_0

$$da(t)/dt = Q_2[a(t)]^{b_2}; \quad a(t) > a_0 \quad (4)$$

The probability of crack exceedance, $p(i, \tau)$, can be derived by growing the initial flaw size distribution given in Eq. (1) using the crack-growth-rate equations given by Eqs. (3) and (4); with the results (see Refs. 12–14 for detailed derivations)

$$p(i, \tau) = P[a(\tau) \geq x_1] = 1 - F_{a(0)}[y(x_1; \tau)] \quad (5)$$

in which $F_{a(0)}(x)$ is the distribution function of EIFS given by Eq. (1), and $y(x_1; \tau)$ is defined in Eqs. (6) and (7) for $b_1 = b_2 = 1$

$$y(x_1; \tau) = x_1 \exp(-Q_1\tau); \quad x_1 < a_0 \quad (6)$$

$$y(x_1; \tau) = (x_1)^{Q_1/Q_2} \exp(\Lambda - Q_1\tau); \quad x_1 > a_0 \quad (7)$$

where

$$\Lambda = [1 - (Q_1/Q_2)] \ln a_0 \quad (8)$$

Similar equations for $y(x_1; \tau)$ for b_1 and $b_2 \neq 1$ are derived elsewhere.¹³ Since the SCGC should be compatible with the EIFS based on Eq. (2), $b_1 = 1$ is used. Further, reasonable fits for the second segment of the SCGC have been obtained using $b_2 = 1$.^{11,13,14}

Let $T(x_1)$ be the time for a crack to reach any given crack size x_1 and $F_{T(x_1)}(\tau)$ be the corresponding cumulative distribution function, i.e., $F_{T(x_1)}(\tau) = P[T(x_1) \leq \tau]$. The distribution function of $T(x_1)$ is the probability that the crack will reach a crack size x_1 before the service time τ . Such a probability is equal to the probability that the crack size $a(\tau)$ at service time τ will exceed x_1 , which is simply the probability of crack exceedance. Hence,

$$F_{T(x_1)}(\tau) = P[T(x_1) \leq \tau] = P[a(\tau) \geq x_1] = p(i, \tau) \quad (9)$$

Consequently, $F_{T(x_1)}(\tau)$ is obtained for any given crack size x_1 by computing the crack exceedance probability, $p(i, \tau)$, at different values of service time τ .

Deterministic-Stochastic Crack-Growth Approach (Approach II)

In this approach, the following stochastic crack growth rate model is used for the second segment of the SCGC where the crack size is larger than a_0

$$da(t)/dt = XQ_2[a(t)]^{b_2}; \quad a(t) > a_0 \quad (10)$$

in which X is a lognormal random variable with a median of one; Q_2 and b_2 are crack-growth rate parameters. Equation (10) accounts for the crack growth rate variability and is referred to as the "lognormal random variable model" proposed by Yang et al.^{20–26}

The probability density function of the lognormal random variable X with a median 1 is given by

$$f_X(u) = \frac{1}{\sqrt{2\pi} u \sigma_z} \exp\left\{-\frac{1}{2} \left[\frac{\ln u}{\sigma_z}\right]^2\right\}; \quad u \geq 0$$

$$= 0; \quad u < 0 \quad (11)$$

in which σ_z is the standard deviation of the normal random variable $Z = \ln X$. Details for estimating σ_z are given elsewhere.^{12–14}

Let T be the time for EIFS, $a(0)$, to reach the reference crack size a_0 . Then, integrating Eq. (3) from $t = 0$ to $t = T$ for $b_1 = 1$, one obtains

$$T = Q_1^{-1} \ln[a_0/a(0)] \quad (12)$$

in which it is understood that $a(T) = a_0$.

In the crack-size region for $a(\tau) > a_0$ (or $\tau > T$), Eq. (10) can be integrated with $b_2 = 1$ from $t = T$ to $t = \tau$ (or from $a(T) = a_0$ to $a(t) = a(\tau)$; with the result

$$T = \tau - (XQ_2)^{-1} \ln[a(\tau)/a_0]; \quad a(\tau) > a_0 \quad (13)$$

A comparable expression for Eq. (13) has been derived elsewhere¹³ for $b_2 \neq 1$. In this investigation $b_2 = 1$ is used since reasonable predictions for the statistical, crack-growth damage accumulation have been obtained with $b_2 = 1$ for a wide range of large crack sizes.^{6,12,14}

Equating Eqs. (12) and (13) leads to the following relation between $a(\tau)$ and $a(0)$

$$a(0) = a_0 \exp(-Q_1\tau)[a(\tau)/a_0]^{\gamma/X}; \quad a(\tau) > a_0 \quad (14)$$

in which

$$\gamma = Q_1/Q_2 \quad (15)$$

For the crack size $a(\tau)$, smaller than a_0 , the relation between $a(\tau)$ and $a(0)$ is obtained by integrating Eq. (3) for $b_1 = 1$ from $t = 0$ to $t = \tau$ as follows:

$$a(0) = a(\tau) \exp(-Q_1\tau); \quad a(\tau) < a_0 \quad (16)$$

When the crack size of interest x_1 is smaller than the reference crack size a_0 , the crack exceedance probability $p(i, \tau)$ is derived as follows

$$p(i, \tau) = 1 - F_{a(0)}[y(x_1; \tau)]; \quad x_1 \leq a_0 \quad (17)$$

where $F_{a(0)}(x)$ is the distribution function of EIFS, $a(0)$, given by Eq. (1) and

$$y(x_1; \tau) = x_1 \exp(-Q_1\tau) \quad (18)$$

When the crack size of interest x_1 is larger than a_0 , the crack exceedance probability, $p(i, \tau)$, for $x_1 > a_0$ is given by^{12,13}

$$p(i, \tau) = 1 - \int_0^\infty F_{a(0)}[G(x_1; \tau|X = u)] f_X(u) du \quad (19)$$

in which the lognormal probability density function $f_X(u)$ is given by Eq. (11) and

$$G(x_1; \tau|X = u) = a_0 \exp(-Q_1\tau)[x_1/a_0]^{\gamma/u} \quad (20)$$

When the Weibull compatible distribution [Eq. (1)] is used for the EIFS, the condition that $F_{a(0)}[G(x_1; \tau|X = u)] = 1$ for $G(x_1; \tau|X = u) > x_u$ should be observed.

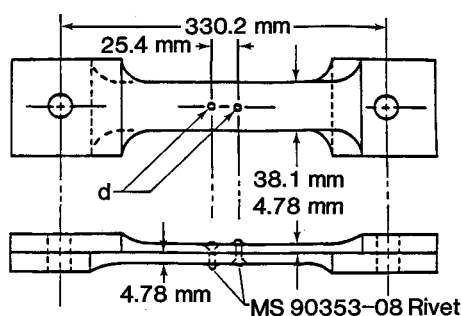


Fig. 2 Double reversed dog-bone specimen with 38.1-mm width and 15% bolt-load transfer.

Table 1 Summary of crack growth parameters for double reversed dog-bone specimen data sets with 15% bolt load transfer

Data sets	No. spec.	σ (MPa)	$Q_1 \times 10^4$ (1/h)
AFXLR4 ^a	10	220.6	2.101 ^c
AFXMR4 ^a	9	234.4	2.514 ^c
AFXHR4 ^a	10	261.9	6.062 ^c
WAFXMR4 ^b	14	234.4	2.906 ^d
WAFXHR4 ^b	12	281.3	3.854 ^d

^aSpecimen details shown in Fig. 2. ^bSpecimen details shown in Fig. 3.

^cFractographic crack-size range used $AL-AU = 0.254 \text{ mm} - 1.27 \text{ mm}$.

^d $AL-AU = 1.27 \text{ mm} - 12.7 \text{ mm}$.

The cumulative distribution of service time $F_{T(x_1)}(\tau)$ for a crack to reach any given crack size x_1 , is determined using Eq. (9). The $F_{T(x_1)}(\tau)$ is obtained for $x_1 < a_0$ and for $x_1 > a_0$ by computing $p(i, \tau)$ at different service times, τ , using Eqs. (17) and (19), respectively.

Durability Analysis Procedures

Durability analysis procedures for implementing the two approaches (see Fig. 1), described above and demonstrated elsewhere,¹²⁻¹⁴ are summarized in the following four steps.

1) Select a reasonable EIFS distribution function $F_{a(0)}(x)$ [e.g., Eq. (1)] and suitable base line fractographic data sets [e.g., Eqs. (18) and (19)]. For each base line fractographic data set, determine the EIFS master curve using 1) fractographic results in a selected crack size range with a lower and upper limit of AL and AU , respectively (e.g., 0.254 mm–1.27 mm); 2) the deterministic, crack-growth rate model [Eq. (2)]; and 3) a least-squares fit procedure.^{13,14} Select a reference crack size a_0 for $AL \leq a_0 \leq AU$ and determine the corresponding time-to-crack-initiation (TTCI) sample values for each data set. Then, for each data set, the EIFS sample value are obtained by back extrapolating the TTCI sample values at a_0 to time zero using the corresponding EIFS master curve.^{13,14}

2) Determine the initial fatigue quality or EIFS distribution for structural details in the durability critical components. Estimate/optimize the EIFS distribution parameters in Eq. (1) using 1) the EIFS sample values from step 1, 2) EIFS data pooling/global least-squares fit procedures, and 3) a statistical scaling technique.¹²⁻¹⁴ Details of this step are given elsewhere.^{13,14} The selected EIFS distribution is justified by checking the goodness-of-fit of crack exceedance predictions for $x_1 \leq AU$.

3) The service, crack-growth master curve in each stress region is determined by either available fractographic results or linear elastic fracture mechanics crack growth analysis. In the latter case, the crack growth computer program is “tuned” or “curve-fitted” to the EIFS master curve in the $AL-AU$ crack size region where base line fractographic data are available. Normal assumptions for the crack shape and geometry are reflected in the crack growth analysis. Then the service, crack-growth master curve is fitted by Eqs. (3) and (4) for

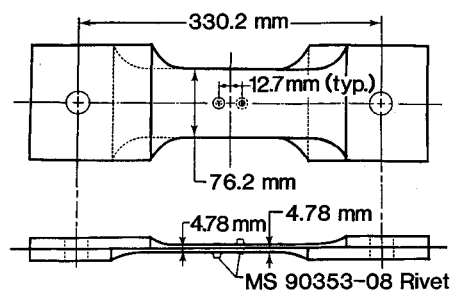


Fig. 3 Double reversed dog-bone specimen with 76.2-mm width and 15% bolt-load transfer.

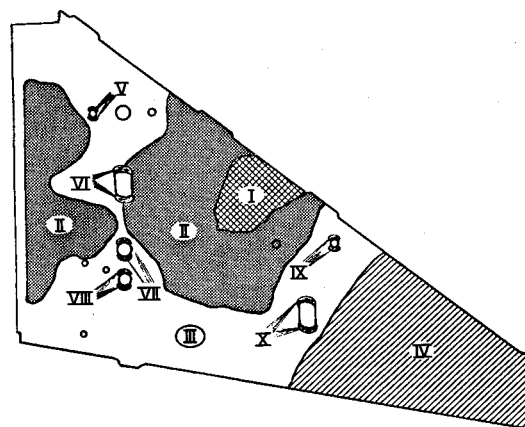


Fig. 4 Stress regions for fighter lower wing skin.

approach I and by the Eqs. (3) and (10) for approach II using a least squares fit procedure.^{13,14} Equation (3) is used to obtain Q_1 for $a(t) < a_0$. For $a(t) > a_0$, Eqs. (4) and (9) are used to estimate Q_2 for approach I and approach II, respectively. The standard deviation σ_z in Eq. (10) can be estimated using available fractographic data or based on past experience.^{13,14}

4) The probability of crack exceedance $p(i, \tau)$ at any service time τ for each stress region i can be determined for approaches I and II using Eqs. (5–7) and (17–20), respectively. Then the statistics for the number of fastener holes that will have a crack size larger than x_1 in the entire durability critical component can be computed using the binomial distribution.^{6,13,14}

The cumulative distribution of service time, $F_{T(x_1)}(\tau)$, to reach any given crack size x_1 can be obtained using Eq. (9) and the applicable $p(i, \tau)$ expressions for approaches I and II, respectively.

Theoretical/Experimental Correlations

Theoretical and experimental correlations for approaches I and II were conducted for clearance-fit countersunk fasteners for full-scale, lower-wing skins of a fighter aircraft. There are several facets to the investigation conducted. Because of space limitations, a brief description of the investigation and the pertinent results obtained are described below. Details are available in Refs. 13 and 14.

The initial fatigue quality of clearance-fit countersunk fasteners (MS 90353-08) in 7475-T7351 aluminum was determined using fractographic results for 38.1 mm-wide, double-reversed, dog-bone specimens with a 15% bolt-load transfer design (see Fig. 2) tested under spectrum loading. Three different fractographic data sets (i.e., AFXLR4, AFXMR4, and AFXHR4)¹⁸ were used to estimate the EIFS distribution parameters for the Weibull compatible distribution function given in Eq. (1). A statistical scaling technique and a data pooling procedure^{13,14} were used to estimate the EIFS distribution parameters in a global sense. The resulting EIFS distribution parameters in Eq. (1) are $x_u = 0.762 \text{ mm}$, $\alpha = 1.716$, and

$\phi = 6.308$. The crack-growth-rate parameter Q_1 for each of the three data sets in the small crack size region, Eq. (3) for $b_1 = 1$, are shown in Table 1. Two fractographic data sets, i.e., WAFXMR4 and WAFXHR4 for 76.2 mm-wide, double-reversed, dog-bone specimens with 15% bolt-load transfer design (see Fig. 3) tested under fighter spectrum loading were obtained to determine the crack-growth-rate parameters in the large crack-size region. The resulting Q_2 values appearing in Eq. (4) for $b_2 = 1$ are presented in Table 1.

The EIFS distribution defined by Eq. (1) and the crack-growth-rate parameters in Table 1 were then used to make $p(i, \tau)$ predictions for the full-scale lower wing skins of a fighter using both crack-growth approaches (see Fig. 1). Analytical predictions and experimental correlations for the lower wing skin are described and discussed in the following sections.

Lower Wing Skins

Fractographic results are available for the lower wing skins from a fighter durability test article¹⁸ that was fatigue tested under spectrum loading to 16,000 flight h. The wing skins are made out of 7475-T7351 aluminum and include countersunk fasteners (i.e., MS 90353-08 blind, pull-through rivets) of the same type used in the test specimens (see Figs. 2 and 3). The durability analysis demonstration was conducted as follows.

1) The EIFS distribution parameters obtained previously for countersunk fastener holes were used for the fighter fastener holes, i.e., $x_u = 0.762$ mm, $\alpha = 1.716$, and $\phi = 6.308$. These parameters were determined from three fractographic data sets,¹⁸ i.e., AFXLR4, AFXMR4, and AFXHR4. Specimen details are shown in Fig. 2.

2) The lower wing skin was divided into ten stress regions as shown in Fig. 4. The maximum stress level σ_i and the number of fastener holes N_i in each stress region are shown in Table 2. Service crack-growth-rate parameters Q_1 and Q_2 ($b_1 = b_2 = 1$) for each stress region in both the small and large crack size regions were estimated using five fractographic data sets de-

scribed in Table 1 and a crack-growth model proposed by Yang and Manning.^{6,13,14}

$$Q_1 = \xi \sigma_i^\psi \quad (21)$$

In Eq. (21), ξ and ψ are empirical constants, which can be determined using either available base-line fractographic data or suitable analytical crack-growth results. In this investigation, fractographic results for three narrow width specimen data sets (i.e., AFXLR4, AFXMR4, and AFXHR4) were used in Eq. (21) to estimate ξ and ψ in the small crack-size region. Fractographic results for two wide-specimen data sets (i.e., WAFXMR4 and WAFXHR4) were used in Eq. (21) to determine ξ and ψ in the large crack-size region. The general approach for estimating ξ and ψ values using the crack-growth-rate parameters presented in Table 1 is conceptually described in Fig. 5. In Fig. 5a for instance, Q_1 values vs the corresponding maximum stress level in Table 1 were plotted in log-log form, and ξ and ψ values were obtained using a linear least-squares procedure.^{6,13,14} The results are given as follows: $\xi = 2.227 \times 10^{-19}$ and $\psi = 6.374$ for $x_1 < a_0$; $\xi = 6.288 \times 10^{-8}$ and $\psi = 1.546$ for $x_1 > a_0$, where $a_0 = 1.27$ mm. Parameter values for ξ and ψ reflect σ_i in MPa units.

Once ξ and ψ are determined from these base-line fractographic data, the crack-growth-rate parameter Q_i in each of the 10 stress regions with a maximum stress level of σ_i is computed from Eq. (21). The resulting crack-growth-rate parameters Q_1 and Q_2 in the small and large crack-size regions for each of the ten stress regions are presented in Table 2.

Table 2 Stress levels, number of fastener holes and crack-growth rate parameters for fighter lower wing skin

Stress region	Max. stress, σ_i (MPa)	No. holes, N_i	Crack-growth parameters $Q_1 \times 10^4$ (1/h)	$Q_2 \times 10^4$ (1/h)
1	195.1	59	0.884	2.187
2	186.1	320	0.655	2.033
3	167.5	680	0.334	1.727
4	115.1	469	0.031	0.967
5	195.8	8	0.904	2.199
6	201.3	30	1.080	2.296
7	223.4	8	2.097	2.697
8	180.6	8	0.541	1.941
9	180.6	12	0.541	1.941
10	177.2	20	0.478	1.885

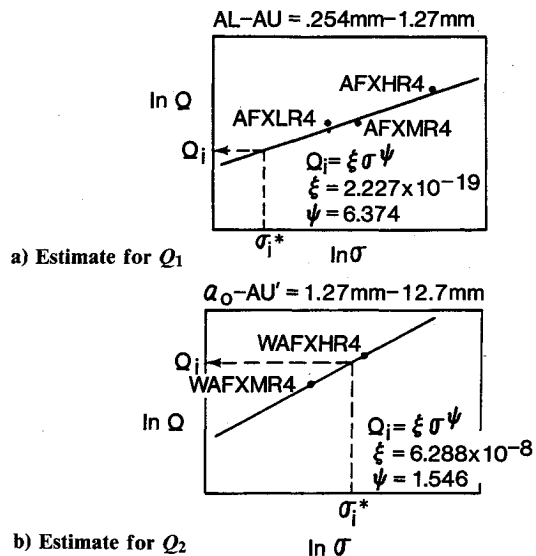


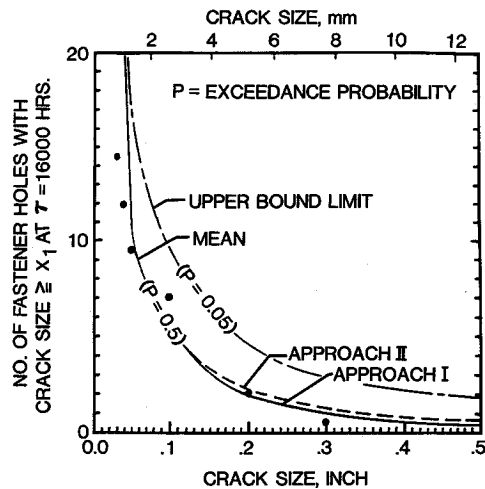
Fig. 5 General approach for estimating service crack-growth parameters Q_1 and Q_2 ; * for each of 10 stress regions, in MPa units.

Table 3 Crack exceedance probability and average number of fastener holes with crack size exceeding x_1 at $\tau = 16,000$ flight h in each stress region based on approach II

Stress Region	$x_1 = 0.762$ mm	$x_1 = 1.27$ mm	$x_1 = 2.54$ mm	$x_1 = 5.08$ mm	$x_1 = 7.62$ mm
	$p(i, \tau)$ $\bar{N}(i, \tau)$	$p(i, \tau)$ $\bar{N}(i, \tau)$	$p(i, \tau)$ $\bar{N}(i, \tau)$	$p(i, \tau)$ $\bar{N}(i, \tau)$	$p(i, \tau)$ $\bar{N}(i, \tau)$
1	0.0739 4.36	0.0350 2.07	0.0183 1.08	0.0071 0.42	0.00348 0.20
2	0.0449 14.37	0.0145 4.64	0.00566 1.81	0.00126 0.40	0.000419 0.13
3	0.0144 9.79	0.0000683 0.05	0.0000066 0.004	0.0000066 0.004	0.0000066 0.004
4	0.000239 0.11	0.00 0.00	0.0000066 0.003	0.0000066 0.003	0.0000066 0.003
5	0.0768 0.61	0.0371 0.29	0.0196 0.16	0.00783 0.06	0.00392 0.03
6	0.103 3.09	0.0577 1.73	0.0335 1.00	0.0158 0.47	0.00894 0.27
7	0.287 2.29	0.225 1.80	0.160 1.28	0.104 0.83	0.0756 0.60
8	0.0326 0.26	0.00714 0.06	0.00187 0.01	0.000196 0.002	0.0000451 0.00
9	0.0326 0.39	0.00714 0.09	0.00187 0.02	0.000196 0.002	0.0000451 0.00
10	0.0264 0.53	0.00403 0.08	0.000621 0.01	0.000031 0.001	0.0000096 0.00
	35.80	10.81	5.377	2.192	1.237

Table 4 Statistics for number of fastener holes with crack size exceeding x_1 in fighter lower wing skin

x_1 (mm)	$\bar{L}(\tau)$	$\sigma_L(\tau)$	Experimental results (Ave.)
0.762	35.80	5.800	14.5
1.27	10.81	3.185	9.5
2.54	5.38	2.262	7.0
5.08	2.19	1.450	1.0
7.62	1.24	1.097	0.5

**Fig. 6** Correlations between theoretical predictions and experimental results for fighter lower wing skin for extent of damage at $\tau = 16,000$ flight h.

3) Typical predictions for crack exceedance probability, $p(i, \tau)$, in each of the 10 stress regions at $\tau = 16,000$ flight h for five different crack sizes (i.e., $x_1 = 0.762$ mm, 1.27 mm, 2.54 mm, 7.62 mm, and 12.7 mm) are shown only for approach II in Table 3 due to space limitations. Analysis details and results for both crack-growth approaches (see Fig. 1) are given in Ref. 14. The analysis for approach II was conducted using $\sigma_z = 0.3$, which is reasonable for countersunk fastener holes in 7475-T7351 aluminum.¹⁴ The average number of fastener holes, $\bar{N}(i, \tau) = N_i p(i, \tau)$, with a crack size $> x_1$ at $\tau = 16,000$ flight h are predicted and shown in Table 3 for each of the ten stress regions. Furthermore, predictions for the average number of fastener holes in the entire lower wing skin with a crack size $> x_1$ at 16,000 flight hours $\bar{L}(\tau)$ and its standard deviation $\sigma_L(\tau)$ are shown in Table 4 for approach II. The $\bar{L}(\tau)$ and $\sigma_L(\tau)$ values are computed based on the binomial distribution^{13,14} as given by Eqs. (22) and (23):

$$\bar{L}(\tau) = \sum_{i=1}^{10} \bar{N}(i, \tau) = \sum_{i=1}^{10} N_i p(i, \tau) \quad (22)$$

$$\sigma_L(\tau) = \left\{ \sum_{i=1}^{10} N_i p(i, \tau) [1 - p(i, \tau)] \right\}^{1/2} \quad (23)$$

Using $\bar{L}(\tau)$ and $\sigma_L(\tau)$, the extent of damage for the lower wing skin can be estimated for selected probabilities. Such results can be used to determine the mean and upper/lower bound limits for the extent of damage.

Theoretical predictions for the average number of fastener holes, $\bar{L}(\tau)$, with a crack size $> x_1$ at $\tau = 16,000$ flight h in the entire lower wing skin are plotted in Fig. 6 for both crack-growth approaches. In this figure, the results for approaches I and II are depicted by a solid curve and a dashed curve, respectively. Results for both approaches are identical for the crack size $x_1 \leq 1.27$ mm = a_0 in the first service crack-growth seg-

ment. The tear-down inspection results are shown in Table 4 and Fig. 6 as solid circles for comparison. These results reflect the average extent of damage for a lower wing skin based on the total extent of damage for left and right lower wing skins combined.

The extent of damage estimate for an exceedance probability of $P = 0.05$ is also plotted in Fig. 6. This curve represents the estimated upper-bound limit for the extent of damage with an exceedance probability $P = 0.05$. It is computed from $\bar{L}(\tau) + 1.65 \sigma_L(\tau)$, where $\bar{L}(\tau)$ and $\sigma_L(\tau)$ values are shown in Table 4 for approach II.

To illustrate the usefulness of the extent of damage concept consider, for example, the extent of damage at $x_1 = 7.62$ mm in Fig. 6. The (predicted) probability of 50% (i.e., $P = 0.5$) means that 1.24 fastener holes will have a crack size exceeding $x_1 = 7.62$ mm; whereas, the probability of 5% (i.e., $P = 0.05$) means 3.05 fastener holes will have a crack size larger than $x_1 = 7.62$ mm at $\tau = 16,000$ flight h. Therefore, the durability analysis provides quantitative estimates for the extent of damage mean and upper-bound limits. This provides a physical description of the state of damage for a durability-critical component and a logical basis for estimating structural maintenance/repair requirements and costs.

It is observed that the durability analysis predictions based on specimen test results correlate well with the tear-down inspections results of the full-scale lower wing skins. Further, the predictions for approach II are slightly more conservative than the results for approach I.

Conclusions

Two different crack-growth approaches for the probabilistic durability analysis have been demonstrated and evaluated using the tear-down inspection results of lower wing skins from a fighter aircraft. Both approaches (i.e., I and II) were evaluated for fatigue cracking in countersunk fastener holes with clearance-fit fasteners. Both two-segment crack growth approaches are considered reasonable for evaluating functional impairment due to fuel leakage/ligament breakage in metallic aircraft structures. However, approach II is recommended for durability analysis because predictions are more accurate and slightly more conservative than those based on approach I.

Acknowledgment

This research was sponsored by the Air Force Wright Aeronautical Laboratories, Wright-Patterson Air Force Base, under Contract No. F33615-84-C-3208.

References

- "Military Specification, Aircraft Structures," Air Force Aeronautical Systems Division, Military Standard MIL-A-87221, Wright-Patterson AFB, OH, Feb. 28, 1985.
- "Aircraft Structural Integrity Program, Airplane Requirements," Air Force Aeronautical Systems Division, Wright-Patterson AFB, OH, Military Standard MIL-STD-1530A, Dec. 1975.
- "Airplane Damage Tolerance Program Requirement," Air Force Aeronautical Systems Division, Wright-Patterson AFB, OH, Military Standard MIL-A-83444, July 1974.
- "Airplane Strength, Rigidity and Reliability Requirement; Repeated Loads and Fatigue," Air Force Aeronautical Systems Division, Wright-Patterson AFB, OH, Military Standard MIL-A-8866B, Aug. 1975.
- Wood, H. A., and Engle, R. M., Jr., "USAF Damage Tolerance Design Handbook: Guidelines for the Analysis and Design of Damage Tolerant Aircraft," Air Force Flight Dynamics Lab., Wright-Patterson AFB, OH, AFFDL-TR-79-3021, March 1979.
- Manning, S. D., and Yang, J. N., "USAF Durability Design Handbook: Guidelines for the Analysis and Design of Durable Aircraft Structures," 2nd ed., Air Force Wright Aeronautical Laboratories, Wright-Patterson AFB, OH, AFWAL-TR-83-3027, Feb. 1989.
- Rudd, J. L., Yang, J. N., Manning, S. D., and Garver, W. R., "Durability Design Requirements and Analysis for Metallic Airframes," *Design of Fatigue and Fracture Resistant Structures*, edited by P. R. Abelkiss and C. M. Hudson, American Society for Testing and Materials, ASTM STP 761, 1982, pp. 133-151.

⁸Rudd, J. L., Yang, J. N., Manning, S. D., and Yee, B. G. W., "Damage Assessment of Mechanical Fastened Joints in the Small Crack Size Range," *Proceedings of the Ninth U.S. National Congress of Applied Mechanics, Symposium on Structural Reliability and Damage Assessment*, Cornell University, Ithaca, NY, June 1982, pp. 329-338.

⁹Rudd, J. L., Yang, J. N., Manning, S. D., and Yee, B. G. W., "Probabilistic Fracture Mechanics Analysis Methods for Structural Durability," *Proceedings of the Conference on the Behavior of Short Cracks in Airframe Components*, AGARD-CP-328, Toronto, Canada, Sept. 1982, pp. 10-1-10-23.

¹⁰Yang, J. N., Manning, S. D., and Rudd, J. L., "Evaluation of a Stochastic Initial Fatigue Quality Model for Fastener Holes," *Fatigue in Mechanically Fastened Composite and Metallic Joints*, edited by John M. Potter, American Society for Testing and Materials, Philadelphia, ASTM STP 927, 1986, pp. 118-149.

¹¹Yang, J. N., Manning, S. D., Rudd, J. L., and Artley, M. E., "Probabilistic Durability Analysis Methods for Metallic Airframes," *Journal of Probabilistic Engineering Mechanics*, Vol. 1, No. 4, Dec. 1981.

¹²Yang, J. N., Manning, S. D., Rudd, J. L., Artley, M. E., and Lincoln, J. W., "Stochastic Approach for Predicting Functional Impairment of Metallic Airframes," *Proceedings of the 28th AIAA/ASME/ASCE/AHS Structures, Structural Dynamics and Materials Conference*, Paper No. 8707520CP, April 1987, pp. 215-223.

¹³Manning, S. D., and Yang, J. N., "Advanced Durability Analysis, Volume I - Analytical Methods," Air Force Wright Aeronautical Laboratories, Wright-Patterson Air Force Base, OH, AFWAL-TR-86-3017, July 1987.

¹⁴Manning, S. D., and Yang, J. N., "Advanced Durability Analysis, Volume II - Analytical Predictions, Test Results and Analytical Correlations," Air Force Wright Aeronautical Laboratories, Wright-Patterson Air Force Base, OH, AFWAL-TR-86-3017, Aug. 1988.

¹⁵Yang, J. N., Manning, S. D., and Garver, W. R., "Durability Methods Development Volume V - Durability Analysis Methodology Development," Air Force Wright Aeronautical Laboratories, Wright-Patterson Air Force Base, OH, AFFDL-TR-3118, Sept. 1979.

¹⁶Yang, J. N. and Manning, S. D., "Distribution of Equivalent

Initial Flaw Size," *1980 Proceedings of Annual Reliability and Maintainability Symposium*, Jan. 1980, pp. 112-120.

¹⁷Yang, J. N., "Statistical Estimation of Economic Life for Aircraft Structures," *Journal of Aircraft*, Vol. 17, No. 7, July 1980, pp. 528-535.

¹⁸Speaker, S. M., et al., "Durability Methods Development, Volume VIII - Test and Fractography Data," Air Force Flight Dynamics Laboratory, Wright-Patterson Air Force Base, OH, AFFDL-79-3118, Nov. 1982.

¹⁹Gordon, D. E., Kirschner, S. B., Brubaker, L. E., Koepsel, K., Manning, S. D., and Yang, J. N., "Advanced Durability Analysis, Volume III - Fractographic Data," Air Force Flight Dynamics Laboratory, Wright-Patterson Air Force Base, OH, AFWAL-TR-86-3017, Aug. 1, 1986.

²⁰Yang, J. N., Salivar, G. C., and Annis, C. G., "Statistical Modeling of Fatigue Crack Growth in a Nickel-Based Superalloy," *Journal of Engineering Fracture Mechanics*, Vol. 18, No. 2, June 1983, pp. 257-270.

²¹Yang, J. N. and Donath, R. C., "Statistical Fatigue Crack Propagation in Fastener Holes Under Spectrum Loading," *Journal of Aircraft*, Vol. 20, No. 12, Dec. 1983, pp. 1028-1032.

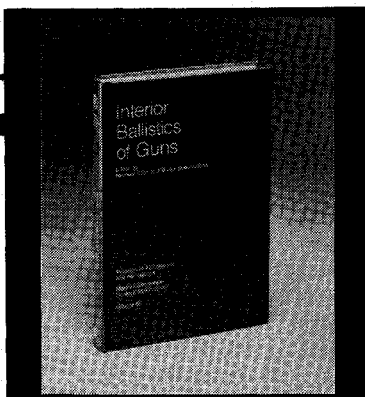
²²Yang, J. N., Manning, S. D., Rudd, J. L., and Hsi, W. H., "Stochastic Crack Propagation in Fastener Holes," *Journal of Aircraft*, Vol. 22, No. 9, Sept. 1985, pp. 810-817.

²³Yang, J. N. and Chen, S., "Fatigue Reliability of Gas Turbine Engine Components Under Schedule Inspection Maintenance," *Journal of Aircraft*, Vol. 22, No. 5, May 1985, pp. 415-422.

²⁴Yang, J. N. and Chen, S., "An Exploratory Study of Retirement-for-Cause for Gas Turbine Engine Components," *Journal of Propulsion and Power*, Vol. 2, No. 1, Jan. 1986, pp. 38-49.

²⁵Yang, J. N., Hsi, W. H., Manning, S. D., and Rudd, J. L., "Stochastic Crack Growth Models for Applications to Aircraft Structures," *Probabilistic Fracture Mechanics and Reliability*, edited by J. W. Provan, Martinus Nijhoff, The Netherlands, 1987, pp. 171-211.

²⁶Yang, J. N. and Chen, S., "Fatigue Reliability of Structural Components Under Scheduled Inspection and Repair Maintenance," *Probabilistic Methods in Mechanics of Solids and Structures*, edited by S. Eggwertz and C. C. Lind, Springer-Verlag, Berlin, 1985, pp. 103-110.



Interior Ballistics of Guns

Herman Krier and
Martin Summerfield, editors

Provides systematic coverage of the progress in interior ballistics over the past three decades. Three new factors have recently entered ballistic theory from a stream of science not directly related to interior ballistics. The newer theoretical methods of interior ballistics are due to the detailed treatment of the combustion phase of the ballistic cycle, including the details of localized ignition and flame spreading; the formulation of the dynamical fluid-flow equations in two-phase flow form with appropriate relations for the interactions of the two phases; and the use of advanced computers to solve the partial differential equations describing the nonsteady two-phase burning fluid-flow system.

To Order, Write, Phone, or FAX:



Order Department

American Institute of Aeronautics and Astronautics
370 L'Enfant Promenade, S.W. ■ Washington, DC 20024-2518
Phone: (202) 646-7444 ■ FAX: (202) 646-7508

1979 385 pp., illus. Hardback
ISBN 0-915928-32-9
AIAA Members \$49.95
Nonmembers \$79.95
Order Number: V-66

Postage and handling \$4.50. Sales tax: CA residents add 7%, DC residents add 6%. Orders under \$50 must be prepaid. Foreign orders must be prepaid. Please allow 4-6 weeks for delivery. Prices are subject to change without notice.